Research Article

Ubiquitin Receptor-Induced Proximity is Sufficient for Ubiquitin-Independent Targeted Protein Degradation via the 26S Proteasome

Seh Hoon Park,[1,2,7] Yejin Jang,[1,2,7] Eunseo Kim,[1,2,4] Dawon Jeong,[1,2] Insuk Byun,[1,2] Jiseong Kim,[1,2] Jisoo Yang,[2,5] Chang Han Lee,[2,5] Dohyun Han,[4] Min Jae Lee[1,2,6]*

[1]Department of Biochemistry and Molecular Biology, Seoul National University College of Medicine, Seoul 03080, Korea

[2]Department of Biomedical Sciences, Seoul National University Graduate School, Seoul 03080, Korea

[3]Department of Biotechnology, The Catholic University of Korea, Bucheon 14662, Korea

[4]Proteomics Core Facility, Biomedical Research Institute, Seoul National University Hospital, Seoul 03080, Korea

[5]Department of Pharmacology, Seoul National University College of Medicine, Seoul 03080

[6]Ischemic/Hypoxic Disease Institute, Convergence Research Center for Dementia, Medical Research Center, Seoul National University, Seoul 03080, Korea

[7]These authors contributed equally to this work.

*Correspondence should be addressed to M.J.L. (minjlee@snu.ac.kr)

Running title: Ub-independent degraders leveraging proteasomal Ub receptors

ABSTRACT

The 26S proteasome engages with ubiquitinated substrates primarily through its constituent ubiquitin (Ub) receptors, which initiates a cascade of events that unfold, translocate, and hydrolyze them. Leveraging this recognition mechanism, we developed a targeted protein degradation (TPD) strategy that recruits substrates directly to the proteasome, bypassing the ubiquitination step. Our proteasome-targeting chimera, Protea-Tac, is a heterobifunctional protein degrader composed of a Ub receptor (PSMD4/Rpn10 or ADRM1/Rpn13) and a target-specific, intracellular antibody (single-chain variable fragment or nanobody). This chimera integrates into 26S proteasomes without altering their structural or functional integrity. Localization of target proteins, including c-Fos, BRD4, Flag-TDP43, HA-tau, and GFP-ODC, to the proteasome via Protea-Tac with cognate antibodies resulted in their induced degradation. We demonstrated that this platform is 1) modular, requiring both essential components but allowing for facile switching between targets; 2) Ub-independent through direct proteasomal targeting; and 3) highly target-specific. Protea-Tac degraded c-Fos *in vivo* and substantially delayed tumor growth in mouse xenograft models. Overall, these findings identify Protea-Tac as a distinct TPD modality capable of direct proteasomal degradation of intracellular proteins.

Keywords: proteasome; Protea-Tac; single-chain variable fragment; targeted protein degradation; ubiquitin; ubiquitin receptor

INTRODUCTION

Targeted protein degradation (TPD) has evolved from a conceptual framework to a viable therapeutic modality that selectively eliminates disease-related proteins.[1] Unlike conventional small-molecule drugs that typically rely on high-affinity binding, TPD can accomplish a catalytic mechanism that allows for effective protein turnover at moderate-to-low binding affinity.[2,3] Proteolysis-targeting chimera (PROTAC) is at the forefront of TPD therapeutics. It is a synthetic heterobifunctional molecule of a target (neo-substrate with shortened half-lives) binder and a ligand for a cellular E3 ubiquitin (Ub) ligase. The induced proximity via PROTAC promotes substrate polyubiquitination (hereafter referred to as ubiquitination) and, subsequently, degradation by 26S proteasomes.[4-8] Many other TPD platforms, including molecular glue degraders (MGDs), employ a similar mode of action to PROTACs.[9-11] These approaches offer distinct advantages over traditional therapeutics, particularly in targeting previously thought-to-be undruggable proteins, such as scaffold proteins, transcription factors, and membrane proteins.[12,13] Additionally, TPD has the potential to provide a durable therapeutic solution for acquired drug resistance often caused by mutations in neoplastic targets.[14-17]

The key mechanistic basis of these TPD modalities is their exploitation of the endogenous Ub-proteasome system (UPS), the primary proteolytic pathway in all eukaryotes.[18] In the UPS, E3 Ub ligases, which have over 600 members encoded in the human genome, serve as the critical regulator of substrate specificity, mediating the proximity between substrates and Ub moieties (charged by E2 Ub-conjugating enzymes). Both PROTACs and MGDs aim to emulate this biochemical process by forming an induced ternary complex in precise spatial proximity and orientation. Nevertheless, finding suitable ligands for target-E3 ligase engagement remains

challenging, particularly for recalcitrant proteins lacking well-defined hydrophobic pockets or possessing intrinsically disordered regions. The development process typically consists of multiple iterative cycles of chemical design, synthesis, functional validation, and optimization. The resultant small molecules, however, tend to have high molecular weights (>800 Da) and large polar surface areas, resulting in relatively low solubility and limited cell permeability. The efficacy of Ub inducers is further constrained by the availability of lysine residues on the neo-substrates and the cellular abundance of E3 enzymes; at present, two E3s, CRBN and VHL, account for more than 90% of current PROTACs and MGDs.[19-22]

The proteolytic "processor" in the UPS is the 26S proteasome holoenzyme, which is responsible for the majority of intracellular protein degradation (at least 80% in proliferating cells).[23] Given its high cellular abundance (> 200 nM) in most cell types,[24-27] the proteasome is an ideal degradation machinery for TPD. Moreover, 26S proteasomes appear to have reserved proteolytic capacity for neo-substrates, since a ~30% decline in 26S proteasome levels after *PSMD2* knockdown did not significantly affect global protein turnover.[28-30] The 26S proteasome is composed of two distinct sub-complexes: the 20S catalytic particle (CP) and the 19S regulatory particle (RP), which can reversibly associate and dissociate in response to cellular stress.[31-33] The 26S proteasome also exemplifies an evolutionary dichotomy; the ancient CP for proteolysis and the billions of years later evolved RP for Ub recognition and processing.[34] Most Ub chains are recognized by Ub receptors (UbRs) located in the RP, including PSMD2/Rpn1, PSMD4/Rpn10, and ADRM1/Rpn13. Interaction between substrates with these subunits initiates a cascade of coordinated processes, including “gate” opening of the CP, conformational remodeling of the RP, and alignment of the RP-CP axial channel allowing efficient substrate translocation.[35-38] Importantly, Ub itself does not possess biological activity or alter substrate

stability; it simply localizes substrates to the 26S proteasome.[39] When the substrate's unstructured region engages with the pore of the PSMC/Rpt ATPase ring, nucleotide hydrolysis generates mechanical force, simultaneously unfolding the substrate and translocating it into the hydrolytic chamber.[40]

To circumvent the mechanistic limitations of E3-dependent TPD strategies, alternative degraders, some of which hijack the lysosomal or autophagic pathways, have been developed.[41-46] In this study, we exploited the biochemical feature of the proteasome-residing UbRs to develop a genetically-encoded, directly 26S proteasome-targeting chimera (Protea-Tac). By fusing PSMD4 or ADRM1 to a substrate-targeting antibody (tAb; single-chain variable fragment [scFv] or nanobody [VHH]), we created a modular degrader system that integrates into 26S proteasomes while preserving their structural integrity and proteolytic activity. Whether Protea-Tac degraders were expressed transiently or permanently in cells, they caused substantial degradation of numerous proteins. Biochemical investigations demonstrated that Protea-Tac is highly modular (i.e., both the UbR and tAb components can be substituted), functionally cooperative (both components are required), and capable of inducing Ub-independent TPD. Multiplexed quantitative proteomics using tandem mass tags (TMTs) revealed its high selectivity. Additionally, *in vivo* experiments showed that Protea-Tac degraders post-translationally reduced target proteins and inhibited tumor growth in mouse xenograft models. This study introduces Protea-Tac as a novel, Ub-independent TPD platform, broadening the therapeutic potential of TPD.

RESULTS

Protea-Tac as a TPD modality that directly engages the 26S proteasome

Based on previous studies, which revealed low micromolar affinity interactions between the UbRs and Ub chains,[47,48] we hypothesized that intracellular antibodies such as scFv and VHH could serve as alternatives to Ub chain-mediated substrate recruitment to the 26S proteasome. We designed the initial Protea-Tac platform by fusing a UbR to an scFv targeting the c-Fos oncoprotein, scFv(c-Fos), at either the N- or C-terminus, so as not to sterically impede the 19S subcomplex assembly (Figure 1A). To assess TPD activity, various Protea-Tac constructs were transiently expressed in A549 cells. We found that PSMD4-scFv(c-Fos) significantly lowered the steady-state levels of co-transfected c-Fos in an expression level-dependent manner (Figure 1B). In sharp contrast, *c-Fos* mRNA levels remained unchanged regardless of co-expression of PSMD4-scFv(c-Fos), LacZ, or their combination (Figure 1C), implying that the reduction in c-Fos protein occurred post-translationally. Chase experiments demonstrated accelerated c-Fos degradation in the presence of its cognate, PSMD4-based Protea-Tac chimera (Figure 1D).

The Protea-Tac degraders with ADRM1 were likewise effective; both ADRM1-scFv(c-Fos) and scFv(c-Fos)-ADRM1 substantially reduced c-Fos protein levels without altering *c-Fos* mRNA (Figures 1E & 1F; Supplementary Figures 1A & 1B). We found that ADRM-based Protea-Tacs were more effective in c-Fos degradation than PSMD4-based degraders (half-lives ($t_{1/2}$) and D_{max} = 1.46 h and 75.1% for scFv(c-Fos)-ADRM1 vs. 2.24 h and 51.9% for PSMD4-scFv(c-Fos)) (Figure 1G; Supplementary Figure 1C). Notably, fusions of scFv(c-Fos) with PSMD2 or other structural components (either CP or RP subunits) of the 26S proteasome did not significantly affect c-Fos levels (Figure 1H; Supplementary Figures 1D–1G). When whole-cell lysates (WCLs) were

subjected to sucrose-gradient ultracentrifugation, immunoblot analysis revealed that PSMD4-scFv(c-Fos) had been incorporated into the 26S proteasome (Supplementary Figure 1H). Next, we performed streptavidin-affinity purification using biotin-hexahistidine (BH)-tagged Protea-Tac constructs, which revealed structurally intact and enzymatically active 26S proteasomes through non-denaturing (native) electrophoresis and in-gel fluorogenic substrate (suc-LLVY-AMC) hydrolysis (Figure 1I; Supplementary Figures 1I–1K). Collectively, these results show that (1) direct substrate tethering to the 26S proteasome is sufficient to trigger TPD and (2) this process can be mediated by specific UbRs, namely PSMD4 and ADRM1.

Having validated Protea-Tac functionality using transient transfection, we next generated stable cell lines overexpressing scFv(c-Fos)-ADRM1 in human breast cancer (MCF7) and colorectal cancer (HCT116) cells, where c-Fos upregulation is implicated in tumorigenesis.[49,50] The selected clones expressing the greatest amounts of scFv(c-Fos)-ADRM1 exhibited marked endogenous c-Fos degradation (72.9% and 58.6% in MCF7 and HCT116, respectively) compared to control cells expressing EGFP (Figure 1J; Supplementary Figure 1L). Again, the mRNA levels of endogenous *c-Fos* remained unaffected (Figure 1K). It was noticeable that both cyclinD1 protein and mRNA levels were substantially reduced in these stable cells (Figures 1J & 1K; Supplementary Figure 1M). Transient expression of scFv(c-Fos)-ADRM1 in MCF7 and HCT116 cells also reduced endogenous c-Fos levels but to a lesser extent than when stably overexpressed (Figures 1L & 1M; Supplementary Figures 1N & 1O), implying that the degradation efficiency of Protea-Tac is largely proportional to its expression levels.

Mechanistic exploration of Ub-independent, proteasomal degradation by Protea-Tac

To understand the mechanistic basis of Protea-Tac-mediated TPD, we first investigated whether

both modules, the tAb and UbR, are necessary and whether their fusion is essential. A panel of control constructs expressing only scFv(c-Fos), UbR alone (PSMD4 or ADRM1), or their co-expression did not affect cellular c-Fos levels, whereas the chimeric Protea-Tac constructs effectively degraded c-Fos (Figures 2A & 2B). As described below, we also achieved successful TPD using VHH as a tAb module, which also showed similar cooperativity between the modules Supplementary Figures 2A & 2B). To further evaluate this cooperativity between modules, we generated constructs that fused scFv(c-Fos) and ADRM1 with or without a self-cleaving T2A sequence at their junction, followed by a P2A-mCherry reporter (Figure 2C). Flow cytometry analysis of A549 cells stably expressing EGFP-tagged c-Fos (EGFP-c-Fos) indicated significantly lower EGFP signals in the mCherry-positive cell population that expresses the fused scFv(c-Fos)-ADRM1 than those expressing the T2A-separated format (Figure 2D).

To further dissect the mechanism and functionality of Protea-Tac, we co-expressed free PSMD4 or ADRM1, which substantially inhibited the TPD activity of Protea-Tac degraders with the cognate UbR module (Figure 2E; Supplementary Figures 2C). In contrast, excess PSMD4 or ADRM1 had no effect on Protea-Tacs with non-cognate UbRs (Figure 2F; Supplementary Figures 2D), demonstrating that Protea-Tac-mediated degradation occurs only within the context of the 26S proteasome holoenzyme and not via monomeric (stand-alone) Ub receptors. Likewise, TPD activity of VHH-based degraders was strongly competed with cognate UbRs (Supplementary Figures 2E & 2F). Protea-Tac chimeras with non-cognate antibodies did not affect c-Fos levels (Supplementary Figures 2G & 2H). We then investigated the impact of tAb affinity on degradation efficiency, using scFv(c-Fos) variants with varying affinities for recombinant c-Fos (Supplementary Figure 2I). We discovered that the lower-affinity T206K mutant improved post-translational c-Fos degradation, whereas the higher-affinity T206E impaired it (Figures 2G & 2H),

suggesting that low-affinity tAbs are sufficient or may be preferable for Protea-Tac-mediated proteasomal TPD to avoid potential "hook" effects.[51]

Because Protea-Tac relies on direct substrate localization to the 26S proteasome rather than ubiquitination, we next sought to investigate its dependency on substrate ubiquitination and proteasomal degradation. The induced degradation of c-Fos and EGFP-c-Fos by PSMD4- or ADRM1-based Protea-Tacs was strongly abrogated by MG132 (a proteasome inhibitor), but not by bafilomycin A1 (an autophagic flux inhibitor) or MLN7243 (an E1 Ub-activating enzyme inhibitor) (Figures 3A & 3B; Supplementary Figures 3A–3D). Similarly, VHH-based Protea-Tac degraders were proteasome-dependent but Ub-independent (Figure 3C & 3D). In chase experiments, treatment with MLN7243 had little effect on EGFP-c-Fos turnover by Protea-Tac but MG132 quickly halted it (Figures 3E–3H). Flow cytometric analysis using EGFP-c-Fos stable cells and chemical inhibitors also revealed that facilitated target degradation by Protea-Tacs was mediated by the 26S proteasome without requiring target ubiquitination (Figure 3I). Overall, these findings establish Protea-Tac as a viable and versatile strategy for engineered protein degradation, serving as the first well-characterized Ub-independent TPD platform.

Versatility and specificity of modular Protea-Tac degraders

To assess the versatility of the Protea-Tac system in targeting diverse neo-substrates, as well as its modular flexibility allowing component substitution, we first replaced the tAb module with scFvs or VHHs that recognize common epitopes such as Flag, HA, or GFP tags (Figure 4A). When expressed in A549 cells, both PSMD4-scFv(Flag) and scFv(HA)-ADRM1 degraders effectively reduced the levels of Flag-TDP43 and HA-Tau proteins, respectively, both in the soluble and insoluble fraction of WCLs, while there was no change in their mRNA levels (Figures 4B–4E;

Supplementary Figures 4A & 4B). In addition, VHH-based chimeras, in which VHH(GFP) was fused to either ADRM1 or PSMD4 showed robust TPD activity toward GFP-tagged ornithine decarboxylase (ODC) (Figures 4F & 4G; Supplementary Figures 4C & 4D). Next, we set out to target BRD4, a protein whose inhibition or depletion has been shown to be therapeutically relevant as an anti-cancer intervention. Consistent with previous observations, the ADRM1-scFv(BRD4) chimera substantially lowered BRD4 protein levels without affecting *BRD4* mRNA expression (Figures 4H & 4I). Collectively, our results indicate that Protea-Tac degraders consistently elicit efficient target degradation by fusing intracellular tAbs to PSMD4 or ADRM1, with varied efficacy depending on target and module. Furthermore, the system displayed high substrate specificity from immunoblotting analyses: scFv(c-Fos) degraders did not affect the stability of Flag-TDP43, HA-Tau, or GFP-ODC, whereas scFv(Flag) or scFv(HA) degraders did not alter c-Fos levels (Figures 4J & 4K; Supplementary Figures 2G, 2H, 4E & 4F).

To evaluate the global impact of Protea-Tac degraders, we performed a quantitative proteomic study using tandem mass tags-mass spectrometry (TMT-MS). Protein samples from five independent cultures transfected with ADRM1-scFv(c-Fos) or individual modules (ADRM1 and scFv(c-Fos) alone) were labeled with isobaric TMT reagents, pooled, fractionated via reverse phase-HPLC, and analyzed using MS^3 methods, identifying a total of 6,295 proteins (Figure 4L; Supplementary Table S1). The principal component analysis revealed two distinct clusters between experimental groups, illustrating the high reproducibility of our TMT-MS analysis (Supplementary Figure 4G). Applying thresholds of > 1.2 log2 fold-change and < 0.05 q-value, only c-Fos and ADRM1 were significantly reduced, while the broader proteome remained largely unchanged (Figure 4M; Supplementary Tables S2 & S3). With the same criteria, 14 proteins (0.22%) were identified to be upregulated but could not be enriched into a hallmark or ontology set. The

pronounced reduction in c-Fos protein levels, as confirmed by both biochemical and TMT-MS assays, underscores the excellent selectivity of the Protea-Tac system, driven by tAb specificity. The decrease in ADRM1 levels is potentially attributable to its inefficient folding when fused to intracellular antibodies[52] (Supplementary Figure 4H). After stable or transient overexpression of Protea-Tac chimeras, there were no noticeable differences in proteasome activity, integrity, or abundance, nor in cellular levels of polyUb conjugates, lysosomes/autophagosomes, or ER stress markers (Figures 4N & 4O; Supplementary Figures 4I–4L). Taken together, these results indicated that modifying proteasomal UbRs with tAb is not only tolerable to the 26S proteasome and the global proteome but also represents a feasible therapeutic method for targeting specific proteins.

In vivo target degradation and anti-tumor efficacy with Protea-Tac

To expand our findings *in vivo*, we evaluated the anti-tumor efficacy of Protea-Tac degraders and the biochemical changes they caused, including their ability to degrade targets in a mouse xenograft model. We employed stably scFv(c-Fos)-ADRM1-overexpressing MCF7 and HCT116 cell lines, as well as their control cells expressing EGFP (Figure 1J; Supplementary Figure 1L), and subcutaneously injected equivalent quantities of these stable cells into six-week-old female NOD/SCID/IL-2γ-receptor-null (NSG) mice. Tumor volumes and body weights were monitored every three days for five to seven weeks. At the experimental end point (days 32 or 52), mice with Protea-Tac-expressing tumors exhibited substantially delayed tumor growth than controls (978.1 ± 285.5 mm^3 in MCF7_EGFP tumors vs. 92.4 ± 18.9 mm^3 in MCF_scFv(c-Fos)-ADRM1 tumors, Figures 5A & 5B; 1244.8 ± 459.8 mm^3 in HCT116_EGFP tumors vs. 176.3 ± 44.8 mm^3 in HCT116_scFv(c-Fos)-ADRM1 tumors, Figures 5G & 5H; $p < 0.0001$, Mann-Whitney U test). In stark contrast, there were no significant differences in body weights between the groups with

MCF7 and HCT116 tumors (Figures 5C & 5I).

Immunoblotting examination of dissected tumor lysates revealed near-complete degradation of c-Fos protein in scFv(c-Fos)-ADRM1-expressing tumors but not in EGFP-expressing controls (Figures 5D & 5J), demonstrating *in vivo* TPD activity of the Protea-Tac system. Furthermore, cyclin D1, a direct transcriptional target of c-Fos, was also significantly reduced, but there were little changes in PARP cleavage (an apoptotic marker) and ERK1/2 and p38 phosphorylation (c-Fos upstream markers) (Figures 5E & 5K; Supplementary Figures 5A & 5B). When we measured mRNA levels from the tumor tissues, *cyclinD1* mRNA expression was significantly downregulated, whereas *Protea-Tac* mRNA expression was highly upregulated, and endogenous *c-Fos* mRNA levels remained unchanged (Figures 5F & 5L; Supplementary Figures 5C & 5D). Flow cytometry analysis of stable cell lines used in xenograft assays also verified a considerable delay in cell cycle progression, particularly at the G1–S transition, in tumors expressing the c-Fos-targeting Protea-Tac degraders (Supplementary Figures 5E & 5F). These findings demonstrate that Protea-Tac degraders have substantial anti-tumor actions *in vivo*, which appear to be mediated predominantly through cell cycle arrest rather than apoptosis activation.

DISCUSSION

The 26S proteasome is the sole ATP-dependent protease in the eukaryotic cytoplasm and nucleus, which uses Ub chains for the recognition of to-be-degraded substrates. Ub chains are primarily used to localize substrates to the 26S proteasome. Unless a substrate lacks a flexible, unstructured region (the "initiation site") that triggers unfolding and translation via the AAA+ PSMC pore loop, this tethering alone is usually sufficient to cause spontaneous substrate hydrolysis in the 20S.[53,54] By harnessing this mechanism, we develop a novel TPD platform by fusing UbRs from the 19S subcomplex to tAbs. This system enables selective proteasomal degradation of intracellular proteins in a Ub-independent manner. As an initial proof-of-concept, we targeted the c-Fos protein (a transcription factor) and further demonstrated the degradation of (TDP43 and tau (aggregation-prone proteins), BRD4 (an oncogenic factor), and ODC (a Ub-independent substrate), using their cognate Protea-Tac degraders. We confirmed that UbR-tAb chimeras were successfully integrated into fully functional 26S proteasomes, and their degradation activity was largely associated with expression levels. Notably, PSMD4 and ADRM1 effectively mediated target degradation, whereas PSMD2 did not. This discrepancy is likely due to positional or orientational biases between neo-substrates and the proteasomal entry pore, rather than Ub linkage topology or receptor binding affinity. Future work is required to determine the preferential UbR-substrate combination for optimal Protea-Tac activity.

Protea-Tac degraders promote proximity-driven, Ub-independent, and proteasome-dependent degradation, making them a compelling alternative to PROTACs and MGs.[55-58] Unlike these conventional degraders, the Protea-Tac system is not limited by the availability of E3 Ub ligases; it can remain functional even in pathological conditions where the components of the Ub-

conjugating pathways are dysregulated.[59] Because Ub chains are not involved in this system, Protea-Tac is resistant to proteasomal deubiquitinating enzymes, such as USP14 and UCH37, which edit the Ub chains and favor substrate release rather than degradation. More importantly, Protea-Tac benefits from highly abundant and ubiquitously expressed 26S proteasomes. The presence of thousands of endogenous (pathophysiological) substrates highlights the extensive proteolytic capabilities of proteasomes and Protea-Tac as well. Our antibody-guided Protea-Tac degraders demonstrated remarkable substrate specificity, as confirmed by global proteomic profiling. As seen in Ub chain-UbR interactions, weak-affinity positioning of neo-substrates to the 19S subcomplex via Protea-Tac appeared sufficient to trigger substrate entry into the 20S catalytic chamber for degradation.[60] Therefore, the scope of Protea-Tac targets is not limited to intracellular antibodies. With continuing advances in antibody and mini-binder engineering,[61] it is expected that a broader repertoire of Protea-Tac degraders than heterobifunctional small molecules will be created to target a wide range of disease-associated proteins, including those lacking small-molecule ligands. Direct proteasomal degradation via Protea-Tac chimeras can be a more general, although not universal, TPD modality.

Despite inherent challenges related to cytosolic delivery and expression, the Protea-Tac platform remains a unique and promising TPD strategy. Its modular architecture allows relatively simple reprogramming for various neo-substrates by switching the tAb component. Using scFv(c-Fos) and targeting c-Fos, we demonstrated a marked delay in tumor growth in MCF7 and HCT116 xenograft models, where c-Fos is a known oncogenic driver. Therefore, Protea-Tac enables direct proteasomal degradation of pathologic proteins *in vivo* and holds potential for therapeutic applications. Future efforts will focus on improving expression systems for *in vivo* applications, validating the platform's versatility as a protein-based therapy. In summary, this study introduces

a modular TPD platform, exploiting an orthogonal Ub delivery mechanism (via the UbR module) and capable of targeting a wide range of substrates (via the tAb module). The Protea-Tac system showed high specificity and potency *in vivo* without the need for target ubiquitination, making it a novel TPD modality.

MATERIAL AND METHODS

Antibodies and Reagents

The following primary antibodies were used: anti-c-Fos (Cell Signaling Technology [CST], 1:2,000 for IB), anti-PSMD4 (Thermo Fisher Scientific [TFS], 1:1,000), anti-ADRM1 (TFS, 1:1,000), anti-PSMA4 (Enzo Life Sciences, 1:1,000), anti-V5 (TFS, 1:3,000), anti-ACTB (MilliporeSigma, 1:3,000), anti-GAPDH (Santa Cruz Biotechnology [SCBT], 1:3,000), anti-MCL1 (CST, 1:2,000), Streptavidin-HRP (MilliporeSigma, 1:1,000), anti-cyclin D1 (CST, 1:2,000), anti-Flag (TFS, 1:1,000), anti-HA (MilliporeSigma, 1:3,000), anti-GFP (SCBT, 1:3,000), anti-PSMC2 (SCBT, 1:1,000), anti-PSMB5 (TFS, 1:1,000), anti-PSMB6 (TFS, 1:1,000), anti-PSMA3 (Enzo Life Sciences, 1:1,000), anti-PSMD1 (SCBT, 1:1,000), anti-LC3B (MilliporeSigma, 1:1,000), anti-Ub (SCBT, 1:3,000), anti-NFE2L1 (TFS, PA5-90023, 1:3,000), anti-p62 (Abcam, ab56416, 1:3,000), anti-LAMP1 (SCBT, sc-20011, 1:1,000), anti-p-IRE1α (Ser724, TFS, PA1-16927, 1:1,000), anti-CHOP (TFS, MA1-250, 1:1,000), anti-p-eIF2a (Abclonal, AP0342, 1:1,000), anti-c-Jun (CST, 9165T, 1:2,000), anti-PARP (TFS, 436400, 1:1,000), anti-ERK1/2 (CST, 4695S, 1:1,000), anti-p-ERK1/2 (CST, 4370S, 1:1,000), anti-p38 (CST, 8690T, 1:1,000), and anti-p-p38 (CST, 4511T, 1:1,000). Secondary antibodies included HRP-conjugated anti-mouse IgG, anti-rabbit IgG, and anti-rat IgG (all from TFS, used at 1:10,000 for IB). Sources of major biochemical reagents are as follows: MG132 (AG Scientific), MLN7243 (Cayman Chemical), Bafilomycin A1 (Cayman Chemical), suc-LLVY-AMC (Bachem), and No-Stain™ Protein Labeling Reagent (TFS). All scFvs and VHHs were derived from plasmids deposited at Addgene (182090, 198303, 198302, and 166518).

Mammalian cell culture and transient expression

Mammalian cell lines used in this study, including A549, HCT116, MCF7, and their derivatives stably expressing EGFP, scFv(c-Fos)-ADRM1, were cultured in RPMI (Wellgene), whereas HEK293T cells were cultured in DMEM (Wellgene), supplemented with 10% heat-inactivated FBS (Gibco), 100 U/mL penicillin, 100 μg/mL streptomycin, and 2 mM L-glutamine. Cells were maintained at 37 °C in a humidified atmosphere containing 5% CO_2. For transient overexpression, cells were seeded to reach approximately 70% confluence and transfected with indicated plasmid DNA using Lipofectamine 3000 (TFS) according to the manufacturer's instructions. The total amount of plasmid DNA was kept constant within each experimental set (2 or 4 μg of total plasmid DNA in a six-well plate). After incubation, cells were washed with PBS and lysed in RIPA buffer (50 mM Tris-HCl [pH 8.0], 1% NP-40, 0.5% deoxycholate, 0.1% sodium dodecyl sulfate [SDS], and 150 mM NaCl) supplemented with protease inhibitor cocktails, or other indicated buffers. WCLs were clarified by centrifugation at 13,000 rpm for 15 min at 4 °C, mixed with 2 × SDS sample buffer, and denatured at 85 °C for 15 min prior to SDS-PAGE and subsequent analyses. For chase analysis, cells were treated with 75 μg/mL cycloheximide at time zero, and samples were collected at indicated chase points.

RNA isolation and quantitative RT-PCR (qRT-PCR)

Total RNA from cultured cells was extracted using TRIzol (Favorgen), followed by additional purification with RNeasy Mini Columns (Qiagen) with on-column DNase I treatment. cDNA synthesis was performed using an RT-PCR premix (Bioneer) and qRT-PCR was conducted using 1/20-diluted cDNA, SYBR qPCR Master Mix (Bioneer), and 10 μM primers. The target gene-specific primer sequences were as follows: for GAPDH, forward 5'-

AGGGCCCTGACAACTCTTTT-3' and reverse 5'-AGGGGTCTACATGGCAACTG-3'; for c-Fos, forward 5'-CACTCCAAGCGGAGACAGAC-3' and reverse 5'-AGGTCATCAGGGATCTTGCAG-3'; for cyclinD1, forward 5'-GCTGCGAAGTGGAAACCATC-3' and reverse 5'-CCTCCTTCTGCACACATTTGAA-3'; for BRD4, forward 5'-ACCTCCAACCCTAACAAGCC-3' and reverse 5'-TTTCCATAGTGTCTTGAGCACC-3'; for TDP-43, forward 5'-GGGTAACCGAAGATGAGAACG-3' and reverse 5'-CTGGGCTGTAACCGTGGAG-3'; for tau, forward 5'-CCAAGTGTGGCTCATTAGGCA-3' and reverse 5'-CCAATCTTCGACTGGACTCTGT-3'; for GFP, forward 5'-AAGCAGAAGAACGGCATCAA-3' and reverse 5'-GGGGGTGTTCTGCTGGTAGT-3'; and for scFv(c-Fos)-ADRM1, forward 5'-CCGAAGATCTGGGAGTGTACT-3' and reverse 5'-CACCAAGTACTTGTTGGAGGC-3', where the scFv primers were designed to specifically amplify the scFv region, avoiding endogenous ADRM1. Gene expression levels were normalized to *GAPDH*, and statistical significance was evaluated using a two-tailed Student's t-test with $p < 0.05$ considered significant.

Soluble/insoluble fractionation and sucrose-gradient ultracentrifugation.

Cells expressing Protea-Tac degraders were washed with ice-cold PBS and lysed in RIPA buffer supplemented with protease inhibitor cocktails. WCLs were centrifuged at 16,000 × g for 30 min at 4 °C to separate supernatants (RIPA-soluble fractions), which were boiled at 85 °C for 15 min in 2 × SDS sample buffer. Pellets (RIPA-insoluble fractions) were washed with lysis buffer, resuspended in SDS sample buffer, and boiled at 100 °C for 15 min. For sucrose-gradient ultracentrifugation, cells were homogenized with 1 mL of buffer A (50 mM NaH_2PO_4 pH 7.5,

10 mM NaCl, 5 mM $MgCl_2$, 5 mM ATP, 1 mM DTT, and protease inhibitor cocktails). After brief centrifugation, the soluble fractions were loaded on top of a pre-set sucrose gradient (12 mL, 10–30%) and centrifuged at 312,000 × g in a Beckman SW-41 Ti rotor for 16 h at 4 °C. The gradients were manually fractionated into 300 μL fractions from top to bottom.

Affinity purification and Native PAGE analysis of 26S proteasomes

For affinity purification using biotin tags, cells were harvested in lysis buffer (25 mM Tris-HCl [pH 7.5], 10% glycerol, 5 μM $MgCl_2$, 1 mM ATP, 1 mM DTT, and protease inhibitor cocktails) and homogenized with a Dounce homogenizer. The lysates were incubated with streptavidin-conjugated agarose beads overnight at 4 °C. The beads were washed five times with wash buffer (20 mM Tris [pH 7.5], 15 % glycerol, 1 mM EDTA, 150 mM KCl, 0.05 % NP-40, 1 mM DTT, and 0.2 mM PMSF). Next, the precipitated proteins were eluted from the resin by incubating in TEV cleavage buffer (50 mM Tris-HCl [pH 7.5], 1 mM ATP, 10% glycerol, and TEV protease) for 3 h at 30 °C. Then, the eluted proteins were concentrated with Amicon Ultra-0.5 centrifugal filter units (MilliporeSigma). Proteins were resuspended in Tris-Glycine Native Sample Buffer (TFS) and resolved on 3–8% NuPAGE Tris-Acetate native gels (TFS) at 150 V for 4–5 h. Gels were incubated in activity assay buffer (20 mM Tris, 1 mM ATP, 5 mM $MgCl_2$) containing 100 μM suc-LLVY-AMC to visualize proteasome complexes. To activate 20S proteasomes in native gels, 0.02% SDS was added. After fluorescence-based in-gel activity assay, separated samples in the gel were transferred to PVDF membranes for IB analysis.

Flow cytometry for c-Fos degradation and cell cycle distribution

EGFP-c-Fos stable cells were transfected with either tricistronic scFv(c-Fos)-T2A-ADRM1-P2A-mCherry or bicistronic scFv(c-Fos)-ADRM1-P2A-mCherry plasmids and incubated for 72 h. Cells were harvested, washed, and resuspended in FACS buffer (0.2 % of BSA, 0.1 % of sodium azide, and 2 mM of EDTA in PBS). Flow cytometry was performed on a BD LSRFortessa X-20 using FITC and PE channels. Data were analyzed using Flowjo software (ver. 10.9.0). For DNA content analysis, EGFP or scFv(c-Fos)-ADRM1 expressing cells were fixed in 70% ethanol overnight, washed, and stained with DAPI/Triton X-100 at RT for 30 min in the dark. Flow cytometry was performed using LSRFortessa (BD Bioscience) with UV excitation at 340 to 380 nm and analyzed using FlowJo to quantify the distribution across G0/G1, S, and G2/M phases.

Affinity tuning of scFv(c-Fos) and affinity measurement

To change the binding affinity of scFv(c-Fos), random mutagenesis of six central residues within the CDR3 region was performed using primers containing NNK degenerate codons. The resulting mutant libraries were cloned into the pMopac12 vector and transformed into *E. coli* Jude1 cells. Individual colonies (N = 596) were cultured in 96-deep-well plates and induced with 0.5 mM IPTG at 20°C for 20 h. Secreted scFv(c-Fos) variants were purified from culture supernatants using Ni-NTA affinity chromatography. To express recombinant GST-tagged c-Fos, *E. coli* BL21(DE3) cells harboring the expression plasmids were induced with 0.5 mM IPTG, followed by incubation at 30°C for 16 h. Cells were lysed, and clarified lysates were applied to a GST-affinity column, eluted with 20 mM reduced glutathione, and buffer-exchanged into PBS using Amicon Ultra centrifugal filters (10 kDa MWCO). Protein purity and molecular weight were verified by SDS-PAGE and protein staining, and concentrations were determined by absorbance at 280 nm using a NanoDrop spectrophotometer.

To assess antibody affinity, purified scFvs (200 ng/well) were coated onto 96-well immunoplates and incubated overnight at 4°C. After blocking with 3% BSA in PBS, serial dilutions of GST-c-Fos (ranging from 5 μM to 0.32 nM) were added to the plates and incubated for 1 h at RT. Plates were then washed with PBST and incubated with HRP-conjugated anti-GST antibodies for additional 1 h at RT. TMB-ELISA substrates (TFS) were then applied for 20 min, and the reaction was stopped by the addition of 2 M H_2SO_4. Absorbance at 450 nm was measured using an Infinite 200 PRO NanoQuant microplate reader. Dose-response curves were generated, and half-maximal inhibitory concentrations (IC_{50}) were calculated from normalized values using GraphPad Prism (ver. 10.4.1).

TMS-MS analysis

Protein samples were prepared from A549 cells after transfection with either ADRM1 and scFv(c-Fos) (control) or scFv(c-Fos)-ADRM1 degraders (Protea-Tac) for 64 h in biological quintuplicates (N = 5 per group). Cells were washed three times with ice-cold PBS, snap-frozen in liquid nitrogen, lysed in freshly prepared MS lysis buffer (4% SDS and 0.1 M Tris-HCl [pH 8.0]), heated at 95°C for 20 min, and sonicated. Lysates were cleared by centrifugation at 15,000 rpm for 20 min at room temperature (RT), and protein concentrations were determined using a BCA assay (TFS). An aliquot containing 40 μg of total protein per sample was precipitated in pre-chilled acetone at −20°C overnight and collected by centrifugation at 14,000 rpm for 10 min at 4°C. After air-drying, pellets were resuspended in denaturing buffer (5% SDS, 10 mM TCEP, 50 mM CAA, and 50 mM HEPES [pH 8.5]), reduced, alkylated, and then acidified with phosphoric acid to pH ≤1. Following additional centrifugation, the samples were processed with S-Trap micro columns (Protifi), washed with methanol-containing buffer, and digested on-column with trypsin (1:25 enzyme-to-protein

ratio) at 47°C for 2 h. Peptides were eluted sequentially using three buffers (50 mM HEPES; 0.2% formic acid in water; and 0.2% formic acid in 50% acetonitrile), pooled, and dried under vacuum. The resulting peptides were labeled using TMTpro 16plex reagents (TFS; Lot #XL348283) according to the manufacturer's instructions. After labeling for 15 min and quenching with 5% hydroxylamine, labeled peptides were combined in equal amounts across all channels, desalted using Sep-Pak tC18 cartridges (Waters), and dried again by vacuum centrifugation. To reduce ratio compression and systematic bias, the TMT channels were systematically assigned rather than randomized: HEK293T reference (channel 126), controls (127N–131C), and Protea-Tac groups (132N–134N). Pooled peptides were fractionated under high-pH conditions using an Agilent 1260 HPLC system equipped with a ZORBAX 300Extend-C18 column (4.6 mm × 150 mm, 3.5 µm; Agilent). Peptides were separated using a 55-min gradient, increasing buffer B (15 mM ammonium hydroxide in 90% acetonitrile [pH 10.0]) from 5% to 35% over 43 min at a flow rate of 0.2–1.0 mL/min. Ninety-six fractions were collected and concatenated into 24 fractions, which were vacuum-dried and stored at −80°C until MS analysis.

For LC-MS^3 analysis, each fraction was reconstituted in 10 µL of 0.1% formic acid/2% acetonitrile solution, and 2 µL were injected onto a trap column (75 µm I.D. × 2 cm, 3 µm PepMap100 C18 beads) before separation on an EASY-Spray analytical C18 column (75 µm × 50 cm, 2 µm particle size; TFS) using an Ultimate 3000 UHPLC system coupled to a Q-Exactive HF-X mass spectrometer (TFS). A 130-min linear gradient ramping solvent B (0.1% formic acid in acetonitrile) from 8% to 60% was applied at a flow rate of 300 nL/min. MS1 scans were acquired in positive ion mode over a mass range of m/z 350–1,800 at a resolution of 120,000 (FWHM at m/z 200), with an AGC target of 3×10^6 and maximum injection time of 25 ms. The top 15 most intense precursor ions were selected for higher-energy collisional dissociation fragmentation using

a 0.7 Th isolation window, normalized collision energy of 32%, and MS2 scans acquired at 30,000 resolution, with an AGC target of 1×10^5 and maximum injection time of 80 ms. Raw MS data were analyzed using Proteome Discoverer ver. 3.1 (TFS), employing the Sequest HT search engine and Percolator algorithm to control the false discovery rate (FDR) at 1% at both the peptide and protein levels. Spectra were searched against the reviewed human UniProt proteome (March 2024, 20,435 entries) supplemented with common contaminants. Precursor mass tolerance was set at ±10 ppm, and fragment mass tolerance at ±0.02 Da. Peptide-spectrum matches were filtered to include only those with Sequest HT Xcorr ≥1, high Percolator confidence, and reporter ion signal-to-noise ratios >10, with spectra showing isolation interference >70% excluded. Quantification was performed using both unique and razor peptides, applying isotopic impurity correction factors provided by the manufacturer, and proteins identified with fewer than three unique peptides were excluded from further quantitative analysis. The TMT-MS proteomics data have been deposited in the ProteomeXchange Consortium via the PRIDE partner repository with the data set identifier PXD063133.

Tumor xenograft mouse model

All experiments related to animals were performed according to the protocols accredited by the Institutional Animal Care and Use Committee (IACUC) of Seoul National University (IACUC no. SNU-240510-3-2). Mice were housed in a pathogen-free facility fully approved by the Institutional Animal Care and Use Committee (IACUC). EGFP or scFv(c-Fos)-ADRM1 stably expressing cells were suspended in a 1:1 mixture of PBS and Matrigel, and 100 μL of the suspension (5×10^6 cells) was subcutaneously injected into the right flank region of a 6-week-old immunodeficient NOD.Cg-Prkdc^{scid}Il2rg^{tm1Wjl}/SzJ (NSG) mice (The Jackson Laboratory) using a 26-gauge syringe. Tumor

size and body weight were monitored twice a week using a caliper. Tumor volume was calculated using the formula (length × width^2) / 2. When the tumor of EGFP expressing cells reached approximately 1000 mm^3, every mouse was sacrificed and the tumor tissues were removed for subsequent biochemical analyses.

Statistical analysis

Statistical significance between groups was assessed using an unpaired t-test, one-way ANOVA, or two-way ANOVA followed by Tukey's and Sidak's multiple comparison tests as post hoc analyses (GraphPad Prism, ver. 10.4.1). A p-value of less than 0.05 was considered statistically significant. For TMT-MS, protein abundance data were processed in Perseus (ver. 1.6.15.0). Reporter ion intensities were $\log_2$-transformed, and width adjustment normalization was applied to equalize interquartile ranges across samples. Principal component analysis was conducted to visualize overall sample variation and to assess the separation between controls and experimental groups. Student's t-test was performed to identify differentially expressed proteins, applying a Benjamini-Hochberg FDR threshold < 0.05 and a fold-change (FC) cutoff of >1.2 or <0.833, corresponding to a 20% increase or decrease in expression ($|\log_2 FC| > 0.263$).

COMPETING INTERESTS

S.H.P., Y.J, and M.J.L. have filed a patent application through Seoul National University based on this work.

AUTHOR CONTRIBUTIONS

S.H.P. and Y.J. designed and carried out most experiments and data analyses unless otherwise stated. E,K. and D.H. performed TMT-MS analysis. I.B., J.K., and D.J. conducted the xenograft experiments, VHH-based Protea-Tac-related works, and FACS analysis, respectively. J.Y. and C.H.L engineered the c-Fos-targeting scFv antibodies. S.H.P., Y.J. and M.J.L. prepared the manuscript. M.J.L. conceived the study and supervised the project.

ACKNOWLEDGEMENTS

This work was supported by the Samsung Research Funding & Incubation Center of Samsung Electronics (SRFC-MA2202-06 to M.J.L.).

Note: The proteomics data have been deposited in the ProteomeXchange Consortium (#PXD063133). All other data are included in the article, Supplementary Data, and Extended Data. The plasmid constructs and reagents used in this study are available on request from the corresponding author.

REFERENCES

1. Zhao, L., Zhao, J., Zhong, K., Tong, A. & Jia, D. Targeted protein degradation: mechanisms, strategies and application. *Signal Transduct Target Ther* **7**, 113 (2022).
2. Han, X. *et al.* Discovery of Highly Potent and Efficient PROTAC Degraders of Androgen Receptor (AR) by Employing Weak Binding Affinity VHL E3 Ligase Ligands. *J Med Chem* **62**, 11218-11231 (2019).
3. Bondeson, D.P. *et al.* Lessons in PROTAC Design from Selective Degradation with a Promiscuous Warhead. *Cell Chem Biol* **25**, 78-87.e75 (2018).
4. Gustafson, J.L. *et al.* Small-Molecule-Mediated Degradation of the Androgen Receptor through Hydrophobic Tagging. *Angew Chem Int Ed Engl* **54**, 9659-9662 (2015).
5. Sakamoto, K.M. *et al.* Protacs: Chimeric molecules that target proteins to the Skp1–Cullin–F box complex for ubiquitination and degradation. *Proceedings of the National Academy of Sciences* **98**, 8554-8559 (2001).
6. Bricelj, A., Steinebach, C., Kuchta, R., Gütschow, M. & Sosič, I. E3 Ligase Ligands in Successful PROTACs: An Overview of Syntheses and Linker Attachment Points. *Frontiers in Chemistry* **9** (2021).
7. Buetow, L. & Huang, D.T. Structural insights into the catalysis and regulation of E3 ubiquitin ligases. *Nature Reviews Molecular Cell Biology* **17**, 626-642 (2016).
8. Ciechanover, A., Orian, A. & Schwartz, A.L. Ubiquitin-mediated proteolysis: biological regulation via destruction. *Bioessays* **22**, 442-451 (2000).
9. Domostegui, A., Nieto-Barrado, L., Perez-Lopez, C. & Mayor-Ruiz, C. Chasing molecular glue degraders: screening approaches. *Chem Soc Rev* **51**, 5498-5517 (2022).
10. Dewey, J.A. *et al.* Molecular Glue Discovery: Current and Future Approaches. *J Med Chem* **66**, 9278-9296 (2023).
11. Ding, Y., Xing, D., Fei, Y. & Lu, B. Emerging degrader technologies engaging lysosomal pathways. *Chem Soc Rev* **51**, 8832-8876 (2022).
12. An, S. & Fu, L. Small-molecule PROTACs: An emerging and promising approach for the development of targeted therapy drugs. *EBioMedicine* **36**, 553-562 (2018).
13. Toure, M. & Crews, C.M. Small-Molecule PROTACS: New Approaches to Protein Degradation. *Angewandte Chemie International Edition* **55**, 1966-1973 (2016).
14. Neklesa, T. *et al.* ARV-110: An oral androgen receptor PROTAC degrader for prostate cancer. *J. Clin. Oncol* **37**, 10.1200 (2019).
15. Flanagan, J. *et al.* Abstract P5-04-18: ARV-471, an oral estrogen receptor PROTAC degrader for

breast cancer. *Cancer research* **79**, P5-04-18-P05-04-18 (2019).

16. Békés, M., Langley, D.R. & Crews, C.M. PROTAC targeted protein degraders: the past is prologue. *Nature Reviews Drug Discovery* **21**, 181-200 (2022).
17. Stevens, D.A. *et al.* Phase 1 study of KT-413, a targeted protein degrader, in adult patients with relapsed or refractory B-cell non-Hodgkin lymphoma. *Journal of Clinical Oncology* **40**, TPS3170-TPS3170 (2022).
18. Sontag, E.M., Samant, R.S. & Frydman, J. Mechanisms and Functions of Spatial Protein Quality Control. *Annual Review of Biochemistry* **86**, 97-122 (2017).
19. Fang, Y. *et al.* Targeted protein degrader development for cancer: advances, challenges, and opportunities. *Trends Pharmacol Sci* **44**, 303-317 (2023).
20. Zheng, N. & Shabek, N. Ubiquitin Ligases: Structure, Function, and Regulation. *Annu Rev Biochem* **86**, 129-157 (2017).
21. Schapira, M., Calabrese, M.F., Bullock, A.N. & Crews, C.M. Targeted protein degradation: expanding the toolbox. *Nature Reviews Drug Discovery* **18**, 949-963 (2019).
22. Bricelj, A., Steinebach, C., Kuchta, R., Gutschow, M. & Sosic, I. E3 Ligase Ligands in Successful PROTACs: An Overview of Syntheses and Linker Attachment Points. *Front Chem* **9**, 707317 (2021).
23. Zhao, J., Zhai, B., Gygi, S.P. & Goldberg, A.L. mTOR inhibition activates overall protein degradation by the ubiquitin proteasome system as well as by autophagy. *Proc Natl Acad Sci U S A* **112**, 15790-15797 (2015).
24. Asano, S. *et al.* Proteasomes. A molecular census of 26S proteasomes in intact neurons. *Science* **347**, 439-442 (2015).
25. Pack, C.G. *et al.* Quantitative live-cell imaging reveals spatio-temporal dynamics and cytoplasmic assembly of the 26S proteasome. *Nat Commun* **5**, 3396 (2014).
26. Choi, W.H. *et al.* Aggresomal sequestration and STUB1-mediated ubiquitylation during mammalian proteaphagy of inhibited proteasomes. *Proc Natl Acad Sci U S A* **117**, 19190-19200 (2020).
27. Tanaka, K. & Ichihara, A. Half-life of proteasomes (multiprotease complexes) in rat liver. *Biochem Biophys Res Commun* **159**, 1309-1315 (1989).
28. Rusilowicz-Jones, E.V., Urbe, S. & Clague, M.J. Protein degradation on the global scale. *Mol Cell* **82**, 1414-1423 (2022).
29. Peth, A., Nathan, J.A. & Goldberg, A.L. The ATP costs and time required to degrade ubiquitinated proteins by the 26 S proteasome. *J Biol Chem* **288**, 29215-29222 (2013).

30. Tsvetkov, P. *et al.* Compromising the 19S proteasome complex protects cells from reduced flux through the proteasome. *Elife* **4** (2015).
31. Finley, D. Recognition and processing of ubiquitin-protein conjugates by the proteasome. *Annu Rev Biochem* **78**, 477-513 (2009).
32. Choi, W.H. *et al.* ECPAS/Ecm29-mediated 26S proteasome disassembly is an adaptive response to glucose starvation. *Cell Rep* **42**, 112701 (2023).
33. Wang, X. *et al.* The proteasome-interacting Ecm29 protein disassembles the 26S proteasome in response to oxidative stress. *J Biol Chem* **292**, 16310-16320 (2017).
34. Collins, G.A. & Goldberg, A.L. The Logic of the 26S Proteasome. *Cell* **169**, 792-806 (2017).
35. Martinez-Fonts, K. *et al.* The proteasome 19S cap and its ubiquitin receptors provide a versatile recognition platform for substrates. *Nature Communications* **11**, 477 (2020).
36. Matyskiela, M.E., Lander, G.C. & Martin, A. Conformational switching of the 26S proteasome enables substrate degradation. *Nat Struct Mol Biol* **20**, 781-788 (2013).
37. Sledz, P. *et al.* Structure of the 26S proteasome with ATP-gammaS bound provides insights into the mechanism of nucleotide-dependent substrate translocation. *Proc Natl Acad Sci U S A* **110**, 7264-7269 (2013).
38. Choi, W.H. *et al.* Open-gate mutants of the mammalian proteasome show enhanced ubiquitin-conjugate degradation. *Nat Commun* **7**, 10963 (2016).
39. Kim, J. *et al.* Targeted protein degradation directly engaging lysosomes or proteasomes. *Chem Soc Rev* **53**, 3253-3272 (2024).
40. Kim, Y.C., Snoberger, A., Schupp, J. & Smith, D.M. ATP binding to neighbouring subunits and intersubunit allosteric coupling underlie proteasomal ATPase function. *Nat Commun* **6**, 8520 (2015).
41. Li, Z. *et al.* Allele-selective lowering of mutant HTT protein by HTT-LC3 linker compounds. *Nature* **575**, 203-209 (2019).
42. Ji, C.H. *et al.* The AUTOTAC chemical biology platform for targeted protein degradation via the autophagy-lysosome system. *Nat Commun* **13**, 904 (2022).
43. Pance, K. *et al.* Modular cytokine receptor-targeting chimeras for targeted degradation of cell surface and extracellular proteins. *Nat Biotechnol* **41**, 273-281 (2023).
44. Zheng, J. *et al.* Bifunctional Compounds as Molecular Degraders for Integrin-Facilitated Targeted Protein Degradation. *J Am Chem Soc* **144**, 21831-21836 (2022).
45. Zhu, C., Wang, W., Wang, Y., Zhang, Y. & Li, J. Dendronized DNA Chimeras Harness Scavenger Receptors To Degrade Cell Membrane Proteins. *Angew Chem Int Ed Engl* **62**, e202300694 (2023).
46. Bashore, C. *et al.* Targeted degradation via direct 26S proteasome recruitment. *Nat Chem Biol* **19**,

55-63 (2023).

47. Shi, Y. *et al.* Rpn1 provides adjacent receptor sites for substrate binding and deubiquitination by the proteasome. *Science* **351** (2016).
48. Husnjak, K. *et al.* Proteasome subunit Rpn13 is a novel ubiquitin receptor. *Nature* **453**, 481-488 (2008).
49. Gui, Y. *et al.* c-Fos regulated by TMPO/ERK axis promotes 5-FU resistance via inducing NANOG transcription in colon cancer. *Cell Death Dis* **15**, 61 (2024).
50. Lu, C. *et al.* cFos is critical for MCF-7 breast cancer cell growth. *Oncogene* **24**, 6516-6524 (2005).
51. Douglass, E.F., Jr., Miller, C.J., Sparer, G., Shapiro, H. & Spiegel, D.A. A comprehensive mathematical model for three-body binding equilibria. *J Am Chem Soc* **135**, 6092-6099 (2013).
52. Donini, M. *et al.* Engineering stable cytoplasmic intrabodies with designed specificity. *J Mol Biol* **330**, 323-332 (2003).
53. Arkinson, C., Dong, K.C., Gee, C.L. & Martin, A. Mechanisms and regulation of substrate degradation by the 26S proteasome. *Nat Rev Mol Cell Biol* **26**, 104-122 (2025).
54. Martinez-Fonts, K. *et al.* The proteasome 19S cap and its ubiquitin receptors provide a versatile recognition platform for substrates. *Nat Commun* **11**, 477 (2020).
55. Mullard, A. First targeted protein degrader hits the clinic. *Nat Rev Drug Discov* (2019).
56. Zhang, L., Riley-Gillis, B., Vijay, P. & Shen, Y. Acquired Resistance to BET-PROTACs (Proteolysis-Targeting Chimeras) Caused by Genomic Alterations in Core Components of E3 Ligase Complexes. *Mol Cancer Ther* **18**, 1302-1311 (2019).
57. Yang, K. *et al.* A Cell-Based Target Engagement Assay for the Identification of Cereblon E3 Ubiquitin Ligase Ligands and Their Application in HDAC6 Degraders. *Cell Chem Biol* **27**, 866-876 e868 (2020).
58. Otto, C. *et al.* Targeting bromodomain-containing protein 4 (BRD4) inhibits MYC expression in colorectal cancer cells. *Neoplasia* **21**, 1110-1120 (2019).
59. Makaros, Y. *et al.* Ubiquitin-independent proteasomal degradation driven by C-degron pathways. *Mol Cell* **83**, 1921-1935.e1927 (2023).
60. Benn, J. *et al.* Aggregate-selective removal of pathological tau by clustering-activated degraders. *Science* **385**, 1009-1016 (2024).
61. Cao, L. *et al.* Design of protein-binding proteins from the target structure alone. *Nature* **605**, 551-560 (2022).

FIGURE LEGENDS

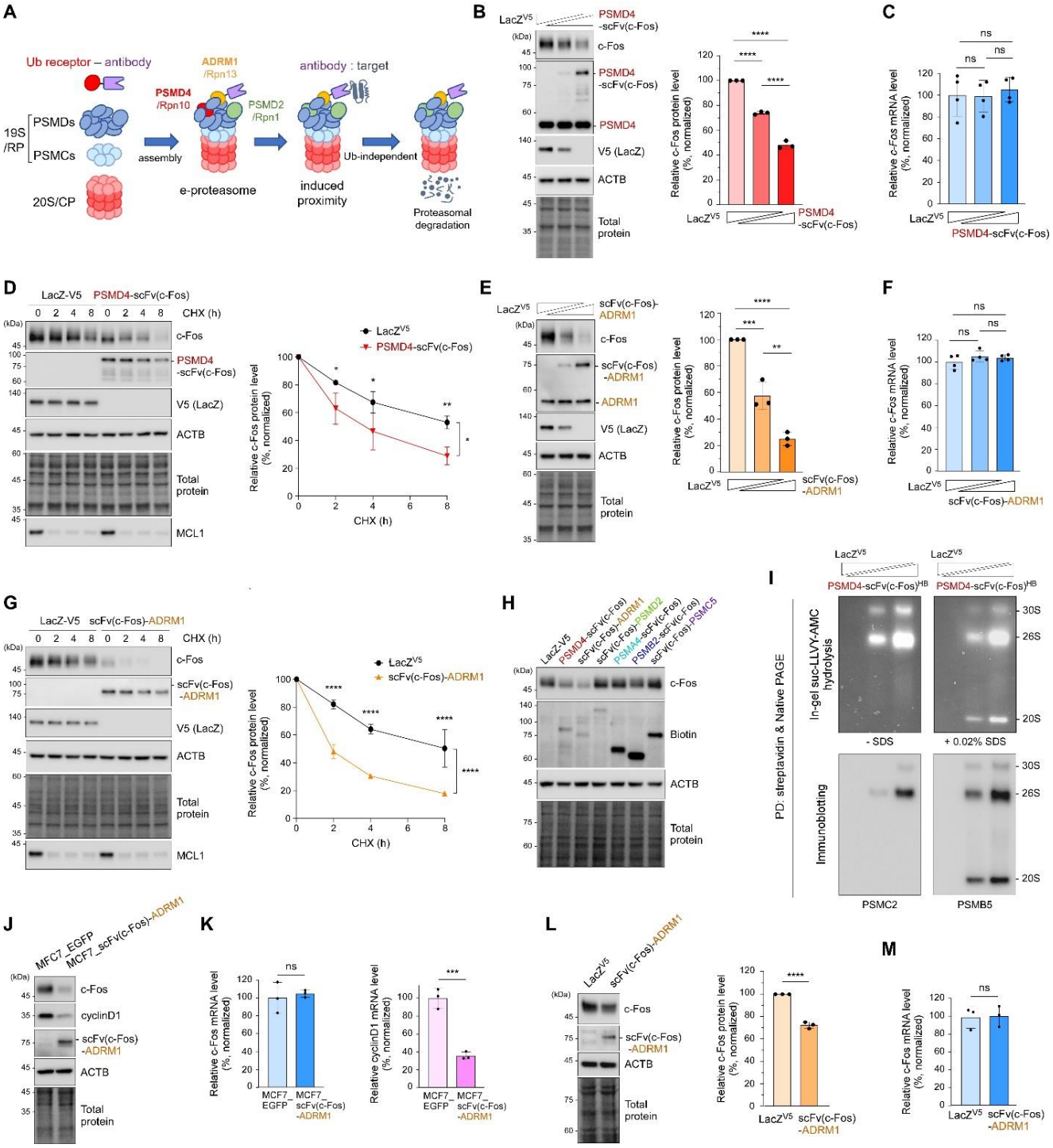

Figure 1. The proteasome-targeting chimera (Protea-Tac) system enables engineered degradation of target proteins through direct proteasome engagement. (**A**) Schematic illustration of targeted protein degradation (TPD) via direct proteasome recruitment by Protea-Tac.

(**B**) A549 cells were co-transfected with plasmids expressing PSMD4-scFv(c-Fos) degraders (0, 0.3, and 1 μg) or $LacZ^{V5}$ controls (1, 0.7, and 0 μg), together with c-Fos-expressing plasmids (0.5 μg). Total plasmid DNA amounts and volumes remained constant across all experimental conditions. After 64 h of incubation, whole-cell lysates (WCLs) were analyzed by SDS-PAGE followed by immunoblotting (IB) and total protein staining. *Left*: Representative IB results from three independent experiments are shown. *Right*: quantification of c-Fos levels normalized to total protein signals. Bars represent the mean ± SD (N = 3). ****$p < 0.0001$ (one-way ANOVA with Tukey's post hoc test). (**C**) As in (B) except total RNA was extracted for quantitative RT-PCR (qRT-PCR) using *c-Fos* and *GAPDH* (normalization control) primers. Values represent the mean ± SD of four independent experiments (N = 4). ns, not significant (one-way ANOVA followed by Tukey's post hoc test). (**D**) Similar to (B) but chase experiments were performed at 2, 4, and 8 h following treatment with 80 μg/mL cycloheximide (CHX) at time zero. c-Fos signals were normalized to the values at 0 h chase (set as 100%) of each group and to total protein levels. Average percentages of remaining c-Fos (mean ± SD) from three independent experiments (N = 3, *$p < 0.05$, **$p < 0.01$ from two-way ANOVA followed by Sidak's post hoc test). MCL1 was used as a physiological proteasome substrate. (**E**–**G**) The ADRM1-based degrader (scFv(c-Fos)-ADRM1) was evaluated in the same methods as in (B–D). (**H**) Various proteasome subunit-based Protea-Tac chimeras were transiently expressed in A549 cells, and c-Fos levels were determined by SDS-PAGE/IB. (**I**) PSMD4-scFv(c-Fos) was tagged with C-terminally hexahistidine-biotin (HB) and transiently expressed for streptavidin affinity purification. Pulldown samples were resolved by native PAGE and analyzed using in-gel suc-LLVY-AMC hydrolysis (*top*) and subsequent IB (*bottom*). The addition of 0.02% SDS activated 20S proteasomes. (**J**) Endogenous c-Fos and cyclinD1 protein levels were compared in MCF7 cells stably expressing EGFP or scFv(c-Fos)-ADRM1. Single-cell clones with the highest expression level were selected for analysis. (**K**) As in (J) except that mRNA levels of endogenous *c-Fos* (left) and *cyclinD1* (right) were evaluated by qRT-PCR and normalized to *GAPDH*. ***$p < 0.001$ (N = 3, two-tailed Student's *t*-test). (**L**) MCF7 cells were transfected with either $LacZ^{V5}$ or scFv(c-Fos)-ADRM1 for 48 h and analyzed for c-Fos levels by IB. Representative blots (*left*) and quantification (*right*) from three independent experiments are shown. (**M**) Similar to (L) but *c-Fos* mRNA levels were evaluated by qRT-PCR analysis. Values are presented as means ± SD. ****$p < 0.0001$ (N = 3, two-tailed Student's *t*-test). ns, not significant. *See* Supplementary Figure 1 and Source Data 1.

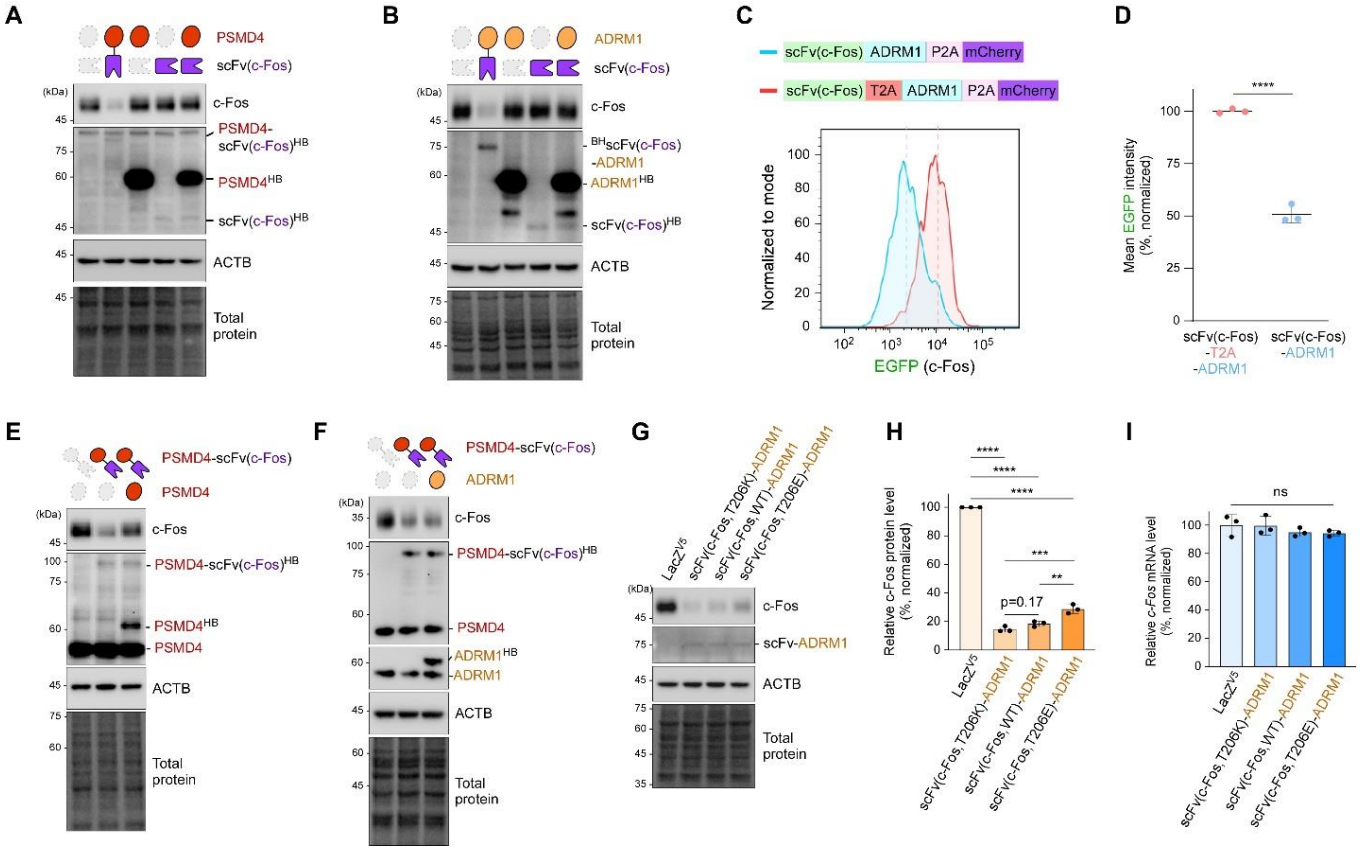

Figure 2. Protea-Tac degraders require both Ub receptor (UbR) and targeting antibody (tAb) for cooperativity.

(**A**) A549 cells were transfected with plasmids expressing PSMD4, scFv(c-Fos), their combination without fusion, or as a PSMD4-scFv(c-Fos) fusion, along with c-Fos-expressing plasmids. LacZ^{V5} plasmids were added to maintain a total plasmid DNA amount (1.5 μg). WCLs were harvested at 64 h post-transfection and examined using SDS-PAGE/IB, followed by total protein staining. (**B**) Same as (A), but ADRM1 was used as the UbR component. (**C**) Schematic of bicistronic (blue) and tricistronic (red) constructs encoding Protea-Tac chimeras with and without T2A peptides at the UbR-tAb junction, respectively. As a reference, mCherry was C-terminally fused via P2A peptides. These constructs were transfected into A549 cells stably expressing EGFP-c-Fos for 72 h, and degradation was monitored using flow cytometry. Representative histograms of EGFP/mCherry ratios from five independent experiments are presented. (**D**) Mean fluorescence intensity (MFI) of EGFP in mCherry-positive cells. Dots indicate the average MFI (normalized)

per experiment, with bars showing the mean ± SD. ****$p < 0.0001$ (N = 3, two-tailed Student's t test). (**E**) As in (A), but PSMD4 was co-expressed with PSMD4-scFv(c-Fos) to assess competitive incorporation into the proteasome and target degradation efficiency. (**F**) ADRM1 (non-cognate UbR) was co-expressed as in (E) to assess competition. (**G**) scFv(c-Fos) variants with lower (T206K) or higher (T206E) binding affinities were evaluated as the tAb component in ADRM1-based degraders. A549 cells were co-transfected with scFv(c-Fos)-ADRM1 (1 μg) or ^{V5}LacZ (1 μg) and c-Fos plasmids (0.5 μg). WCLs were analyzed using SDS-PAGE/IB. Representative IB results from three independent experiments are shown. (**H**) Quantification of c-Fos band intensities from (G), normalized to total protein. Bars indicate the mean ± SD (N = 3). **$p < 0.01$, ***$p < 0.001$, ****$p < 0.0001$ (One-way ANOVA followed by Tukey's multiple comparison test). (**I**) As in (H) except total RNA was extracted for qRT-PCR using *c-Fos* and *GAPDH* (normalization control) primers. Values represent the mean ± SD of four independent experiments (N = 4). ns, not significant (one-way ANOVA followed by Tukey's post hoc test). *See* Supplementary Figure 2 and Source Data 2.

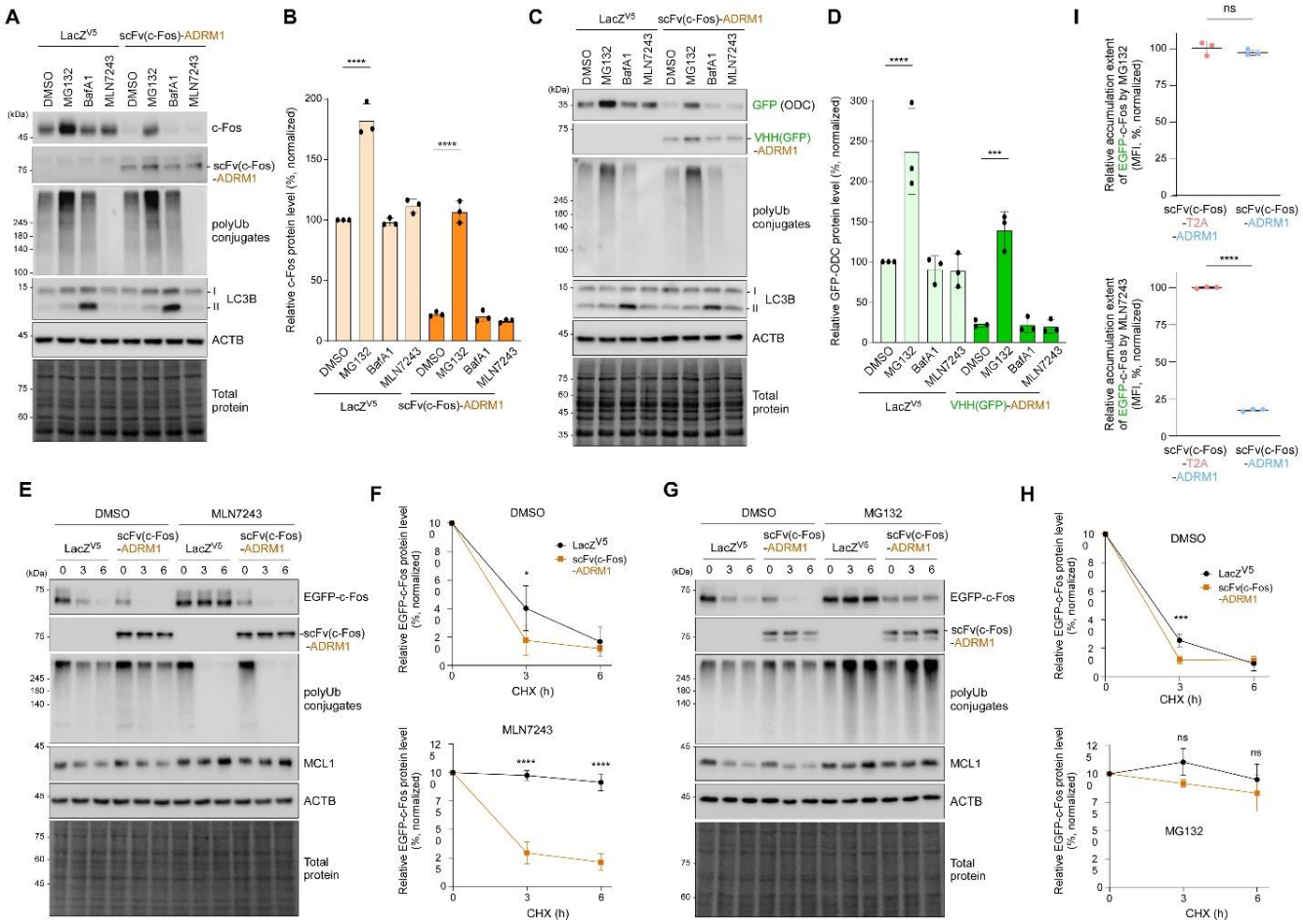

Figure 3. The Protea-Tac system enables Ub-independent and proteasome-mediated TPD. (**A**) scF(c-Fos)-ADRM1-mediated c-Fos degradation was examined in the presence of DMSO, the proteasome inhibitor MG132 (10 μM), the lysosomal vacuolar type H^+-ATPase inhibitor bafilomycin A1 (BafA1; 200 nM), or the E1 Ub-activating enzyme inhibitor MLN7243 (1 μM) for 6 h. (**B**) The steady-state levels of c-Fos detected across conditions in (A) were quantified and normalized to total proteins. Each bar indicates the mean ± SD (N = 3). (**C** & **D**) Identical experiments as panels (A & B), except that VHH(GFP)-ADRM1 was used as a degrader and GFP-ODC was a neo-substrate. (**E**) Chase experiments were performed to track the degradation kinetics of EGFP-tagged versions of c-Fos (EGFP-c-Fos) in the presence of DMSO or MLN7243. (**F**) Quantification of EGFP-c-Fos band intensities in (E), normalized to those of β-actin (ACTB) and to the values at 0 h post-CHX treatment (set as 100%), under DMSO (*top)* or MLN7243 (*bottom*)

treatment conditions. Average percentages of remaining EGFP-c-Fos (mean ± SD) from three independent experiments (N = 3); *$p < 0.05$, ****$p < 0.0001$ (two-way ANOVA followed by Sidak's post hoc test). (**G** & **H**) Chase experiments and quantification using EGFP-c-Fos as in panel (E & F) except they were performed in the presence of either DMSO or MG132. (***$p < 0.001$ (two-way ANOVA followed by Sidak's post hoc test). ns, not significant. (**I**) MFI of EGFP-c-Fos in mCherry-positive cells, determined by FACS analysis. HEK293T stable cells expressing EGFP-c-Fos were treated with either MG132 (*top*: 10 μM for 6 h) or MLN7243 (*bottom*: 1 μM for 6 h) after transfected with bicistronic (blue) and tricistronic (red) Protea-Tac constructs. *See* Supplementary Figure 3 and Source Data 3.

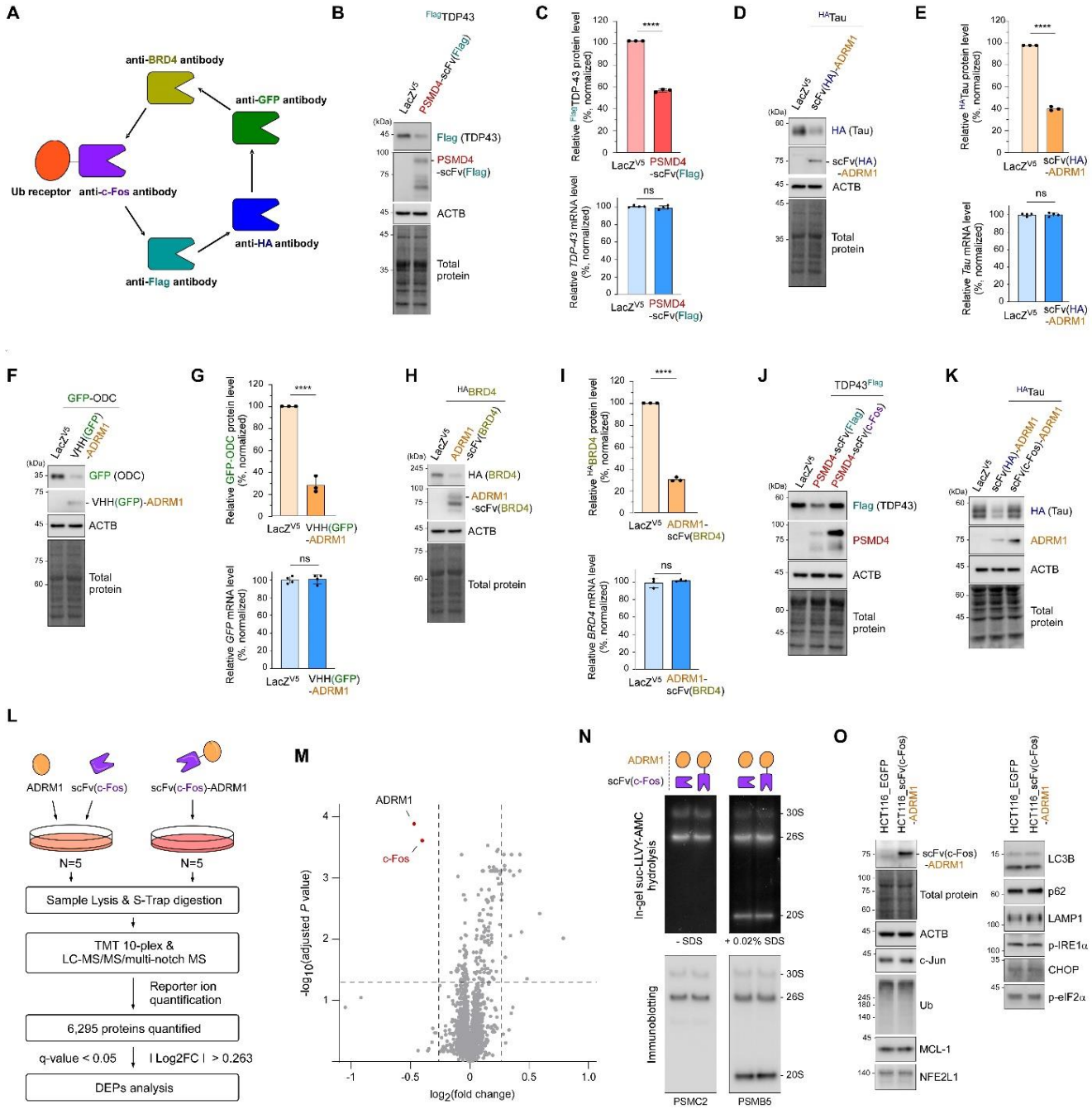

Figure 4. Protea-Tac-mediated degradation is highly selective and modular via UbR and tAb exchanges.

(**A**) Schematic illustrating the modular design of Protea-Tac degraders with interchangeable tAb units. (**B**) A549 cells were co-transfected with ^{Flag}TDP43 and either LacZ^{V5} or the Flag degrader

(PSMD4-scFv(Flag)). After 72 h, WCLs were examined using SDS-PAGE/IB, followed by total protein staining. Representative results from three independent experiments are shown. (**C**) Quantification of ^{Flag}TDP43 protein levels normalization to total protein signals (*top*). Bars indicate the mean ± SD (N = 4). ****$p < 0.0001$ (two-tailed Student's *t*-test). ^{Flag}*TDP43* mRNA levels were measured using qRT-PCR and normalized to *GAPDH.* ns, not significant (N = 4, two-tailed Student's *t*-test). (**D** & **E**) Same as (B & C), except using ^{HA}Tau as the target and scFv(HA)-ADRM1 as the degrader. (**F** & **G**) As in (B & C), except that a nanobody (VHH)-conjugated ADRM1 chimera (VHH(GFP)-ADRM1) was evaluated for degradation of GFP-tagged ODC. (**H** & **I**) Same as (B & C), but with HA-tagged BRD4 oncoprotein (^{HA}BRD4) and ADRM1-scFv(HA). (**J** & **K**) Specificity of Protea-Tac was assessed using mismatched target-degrader pairs. c-Fos-directed Protea-Tac showed no TPD activity toward TDP43^{Flag} (J) and ^{HA}Tau (K). (**L**) Overview of the TMT-MS^3 method for profiling global proteomes. Out of 6,295 identified proteins, 16 differentially expressed proteins (DEPs; 2 downregulated, 14 upregulated) were found in A549 cells treated with ADRM1-scFv(c-Fos) versus controls (ADRM1 + scFv(c-Fos)), using cutoffs of $|\log_2 FC| > 0.263$ and $q < 0.05$. (**M**) Volcano plot of DEPs with dotted lines representing fold-change ($\log_2$) and p-value thresholds. Significantly downregulated DEPa (i.e., c-Fos and ADRM1) are marked in red; upregulated and non-DEPs in gray. (**N**) Native PAGE analysis of 26S proteasomes, followed by in-gel suc-LLVY-AMC hydrolysis visualization (*top*) and subsequent IB with antibodies against the CP (PSMB5) and RP (PSMC2) (*bottom*). The addition of 0.02% SDS activated 20S proteasomes. A549 cells were transfected with either scFv(c-Fos)-ADRM1 plasmid (4 μg) or individual scFv(c-Fos) and ADRM1 plasmids (2 μg each), as in (L). (**O**) Levels of various endogenous proteins in HCT116_EGFP and HCT116_scFv(c-Fos)-ADRM1 stable cell lines were compared using by SDS-PAGE/IB. *See* Supplementary Figure 4 and Source Data 4.

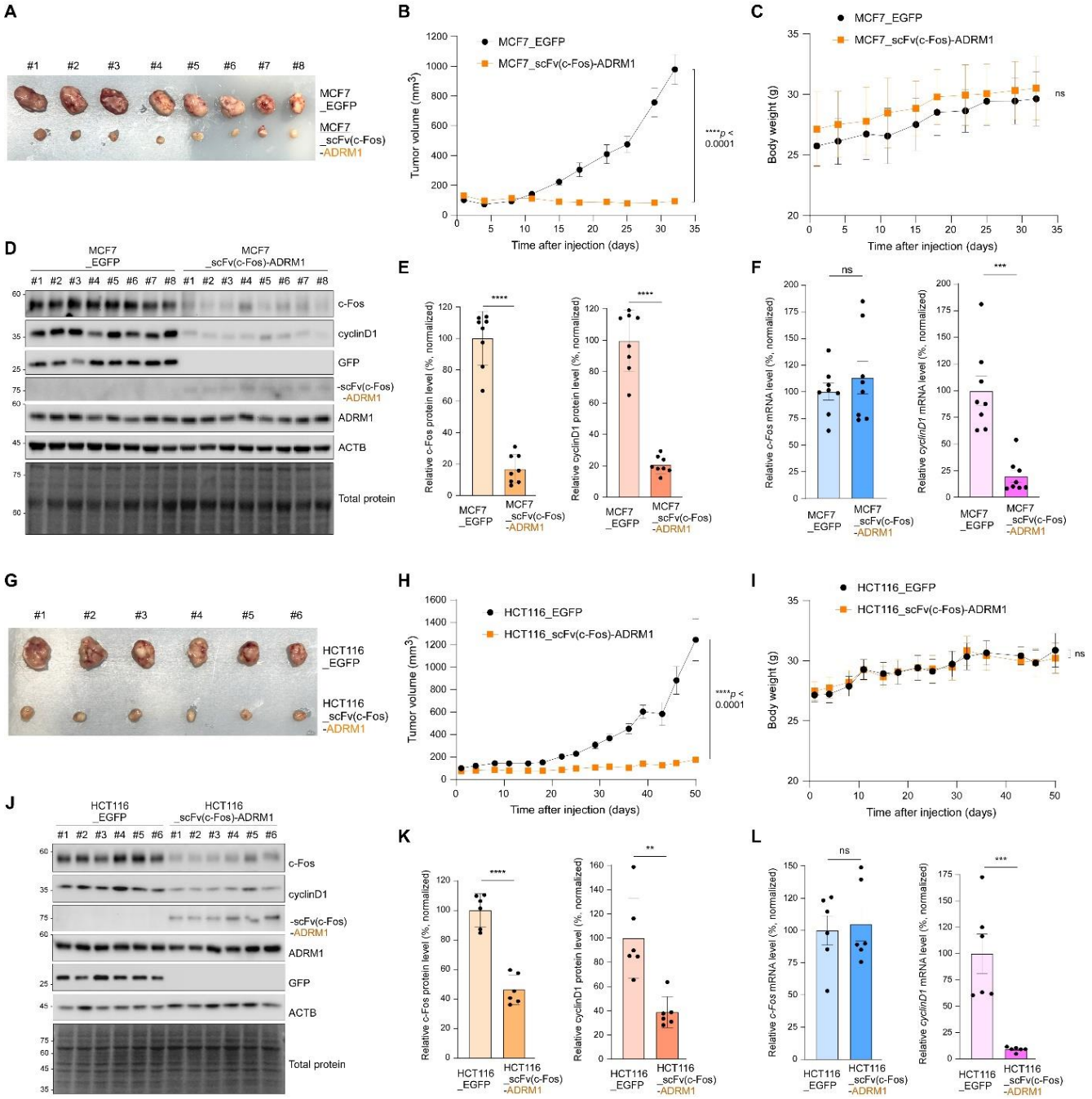

Figure 5. Protea-Tac-induced c-Fos degradation leads to cell cycle arrest and tumor growth inhibition.

(**A**) Images of tumors harvested on day 32 following subcutaneous inoculation of 5×10^6 MCF7 cells stably expressing either EGFP or scFv(c-Fos)-ADRM1 into six-week-old male NOD/SCID/IL-2γ-receptor null (NSG) mice. (**B**) Tumor volumes were measured twice a week for

approximately 5 weeks post-implantation. Data are presented as means ± SEM (N = 8 per group); Mann-Whitney *U* test ($p < 0.0001$). (**C**) Body weight changes during the experiment. (**D**) IB analysis of xenografted tumor lysates showing effective *in vivo* degradation of endogenous c-Fos by the Protea-Tac degrader. (**E**) Quantification of c-Fos (*left*) and cyclinD1 (*right*) protein levels, normalized to total protein signals. Bars represent the mean ± SD (N = 8). ****$p < 0.0001$ (two-tailed Student's t test). (**F**) As in (E), but mRNA levels of *c-Fos* and *cyclinD1* were determined using qRT-PCR and normalized to *GAPDH*. Bars represent the mean ± SEM (N = 8). ***$p < 0.001$ (two-tailed Student's t test). ns, not significant. (**G**) Tumors harvested on day 50 from HCT116_EGFP or HCT116_scFv(c-Fos)-ADRM1 xenografts. (**H**) Tumor volumes measured over approximately 7 weeks. Data are presented as the mean ± SEM (N = 6 for each group) and statistical analysis was performed using the Mann-Whitney *U* test ($p < 0.0001$). (**I** – **L**) Same analyses as in (C–F), using HCT116-derived xenografts expressing EGFP or scFv(c-Fos)-ADRM1. *See* Supplementary Figure 5.